

International Journal of Scientific Research and Reviews

Thermal resistivity and its finite-size scaling in 2D He-4 system

S. Nadim Asghar¹ and Md. Rafiquezaman Ansari^{1*}

¹Department of Physics, J. P. University, Chapra 841301, Bihar, India,
Email: nadimasghar@gmail.com, MobNo. -9934258814

²Department of Physics, Maulana Azad College of Engineering & Technology, Patna 801113, Bihar, India, azamsaba27@gmail.com, MobNo. -8340238097

ABSTRACT

We present a quantitative study of the scaling function which describes the effect of confinement in a cylindrical geometry with radius L on critical properties. The experimental results for the thermal resistivity $\rho(t, P, L) = 1/\lambda(t, P, L)$ near $T_\lambda(P)$ of liquid ^4He confined in cylinders of two different radii and at various pressures as a function of the reduced temperature $t \equiv T/T_\lambda - 1$ have been analyzed. The use of two confinement sizes allows us to directly test finite-size scaling, while the use of different pressures for one size provides a test of universality. For bulk helium $\rho(t, P, \infty)$ depends strongly on pressure, so that a comparison of an appropriate scaling function for $\rho(t, P, L)$ at different pressures provides a sensitive test of universality. These two aspects were tested in separate experiments: measurements as a function of L were taken at SVP, and measurements as a function of were taken at a single confinement size $L = 1.0\mu\text{m}$.

KEYWORDS: Thermal conductivity, Finite-size scaling in 2D He-4 system, Phase transition

*Corresponding author

Dr. Md. Rafiquezaman Ansari

Department of Physics,

Maulana Azad College of Engineering & Technology,

Patna 801113, India

Email: azamsaba27@gmail.com Mob No. -9934258814

INTRODUCTION

The modern theory of critical phenomena¹ predicts that continuous phase transitions belong to distinct universality classes which are determined by such general properties of the system as the number of degrees of freedom of the order parameter and the spatial dimensionality. Within a given class, exponents and amplitude ratios are identical (i.e. universal) for all members and independent of irrelevant variables. An example of an irrelevant variable is the pressure P of a liquid helium sample at which measurements near the superfluid transition temperature T_λ are made. Within a given universality class, the dependence of many properties upon certain parameters can be represented by scaling functions which are the same for all systems.

Theoretical predictions for λ are still quite limited. Monte Carlo calculations give the shape of a scaling function, but only to within a multiplicative factor². Within its precision this shape agrees well with the measurements³. Very recently, a one-loop renormalization group (RG) calculation of $\lambda(t, P, L)$ for $t \geq 0$ and at SVP was carried out by Topler and Dohm⁴, but at present there are no such calculations for $t < 0$ and for higher pressures. Thus, in order to provide a broader framework for the analysis of data, we use a phenomenological approach. We assume that the temperature and size dependence of ρ are separable and that the size dependence is a function only of L/ξ where $\xi = \xi_0 t^{-\nu}$ is the correlation length: $\rho(t, P, L) = \rho(t, P, \infty) \tilde{F}(L/\xi)$. Since $\rho(t, P, \infty)$ goes to zero as t does while $\rho(t, P, L)$ remains finite, \tilde{F} diverges at $t = 0$. To avoid this difficulty, we redefine the scaling function as $F(X) = (L/\xi)^{x/\nu} \tilde{F}$ which avoids the divergence at $t = 0$. Consistent with experiment⁵, we have written ρ for bulk helium as a power law $\rho(t, P, \infty) = \rho_0 t^x$ with effective exponents $x(P)$ and amplitudes $\rho_0(P)$. We now have

$$F(X) = \left(\frac{L}{\xi_0(P)} \right)^{x/\nu} \left[\frac{\rho(t, P, L)}{\rho_0(P)} \right] \quad (1)$$

with

$$X = \left[\left(\frac{L}{\xi_0} \right)^{1/\nu} \right]_t = \frac{t}{t_0} \quad (2)$$

Note that t_0 is the temperature at which the correlation length grows to the size of the container, i.e. $\xi \cong L$. The correlation length has pressure-dependent amplitude $\xi_0(P)$ and a universal exponent ν . The values of ξ_0 , ρ_0 , and x are known from bulk measurements¹ and are summarized in Table 1.

The two different thermal conductivity cells were used. One (Cell I) was described in detail elsewhere³. It was used for measurements of the resistivity as function of P at $L = 1.0 \mu\text{m}$. It

consisted of two cylindrical metal plates made of OFHC (Oxygen-Free High-Conductivity) copper separated by a stainless steel sidewall. A glass micro channel plate (MCP) was epoxied to the inside of the sidewall, so that when assembled the liquid helium between the plates would be confined to the channels with little extraneous liquid between the endplates and the glass. A small bulk thermal conductivity cell, called a “lambda device”, was attached to the bottom (hot) copper plate for the determination of T_λ in bulk helium. The bottom of the lambda device was 1.25 cm below that of the confinement cell, and as a result the value of T_λ had to be corrected for the hydrostatic pressure difference between the bottom of the lambda device and the middle of the MCP^{6,7}. Since the lambda device was attached to the bottom plate, it could only be used before and after a data acquisition sequence because the heat applied to it necessarily flowed through the confining cell. The cell was filled through an overflow volume located on the top (cold) copper plate.

Cell II, used for measurements of the resistivity as a function of L at SVP, was designed for use with micro channel plates which were surrounded by a solid glass ring. Whereas the MCP in Cell I was epoxied into a stainless steel sidewall which in turn was sealed to the copper endplates with indium gaskets, the glass ring in the second type was directly sealed to the copper using indium. A stainless steel sidewall was used as a spacer, but its length was chosen so that the different thermal expansion coefficients of the copper endplates and the stainless steel compensated each other. As a result the force applied to the micro channel plate was constant. The cryogenic apparatus used with this cell design could accommodate three thermal conductivity cells, all of which were suspended from a common temperature-regulated platform. One of these cells was a bulk conductivity cell constructed with an open glass ring. It served to locate T_λ of the bulk fluid. The vertical centers of the cells were nearly the same, so that the gravity correction mentioned for the first cell was greatly reduced. The three cells were independent of each other, so that the bulk thermal conductivity could be measured at the same time as the thermal conductivity for two different confinement sizes. The fill line entered the bottom of the cell, and the portion of the fill line located in the bottom plate was packed with 0.05 μm Alumina powder to suppress the superfluid transition. Thus the liquid helium contained in the bottom plate was always normal. The fill line was connected to an overflow volume on the shield stage, which was maintained a few mK above T_λ .

Saturated vapor pressure was maintained in both sets of experiments by partially filling the overflow volumes. Pressures other than SVP were reached in Cell I using a hot volume⁸, a separate thermal stage filled with fluid whose temperature was controlled to regulate the pressure in the thermal conductivity cell. The pressure was measured using a capacitive strain gage⁹ mounted on

the top of the cell. The fluid in the cell and the hot volume was isolated from the rest of the cryostat by a normally-closed low-temperature valve.

THEORETICAL ANALYSIS

The resistivity ρ was computed from the temperature difference ΔT which was measured across the fluid layer when a power Q was applied to the bottom plate of a cell:

$$\rho = \frac{A}{d} \left(\frac{Q}{\Delta T} - C_w \right)^{-1} - R_b,$$

where A is the cross-sectional area of the fluid, d is the spacing between the plates, C_w is the parallel conductance of the stainless steel sidewall and the glass of the MCP, and R_b is the boundary resistance between the copper end-plates and the fluid. The boundary resistance R_b was measured far below T_λ , where the resistance of the fluid layer can be neglected.

The size of the correction is relatively small, and its temperature dependence near T_λ was neglected.

The parameters A/d and C_w were obtained by fitting the measured $\lambda(t, P, L)$ to the known $\lambda(t, P, \infty)$ several mK above T_λ where the effects of confinement are negligible. For Cell I, the

pressures at which measurements were made were chosen to match those for which prior measurements for bulk helium were available¹; the value $d/A = 0.386$ so obtained was found to be independent of pressure and agreed with the value 0.39 previously determined for this cell³. The 0.5 and 1 μm data, taken with Cell II, yielded $d/A = 0.0781$ and 0.0605, respectively. All values for d/A are in good agreement with values from gas flow-impedance measurements on and electron micrographs of the micro channel plates. The values for C_w for each size and pressure are shown in Table I (for $P = 11.25$ bar, there were no bulk conductivity data, and C_w was obtained by interpolation between other pressures). Each conductivity data point was assigned to the mean temperature $T = T_{top} + \frac{T}{2}$, and a corresponding curvature correction¹ was applied to correct for the use of a finite Q and T .

measurements were made were chosen to match those for which prior measurements for bulk helium were available¹; the value $d/A = 0.386$ so obtained was found to be independent of pressure and agreed with the value 0.39 previously determined for this cell³. The 0.5 and 1 μm data, taken with Cell II, yielded $d/A = 0.0781$ and 0.0605, respectively. All values for d/A are in good agreement with values from gas flow-impedance measurements on and electron micrographs of the micro channel plates. The values for C_w for each size and pressure are shown in Table I (for $P = 11.25$ bar, there were no bulk conductivity data, and C_w was obtained by interpolation between other pressures). Each conductivity data point was assigned to the mean temperature $T = T_{top} + \frac{T}{2}$, and a corresponding curvature correction¹ was applied to correct for the use of a finite Q and T .

Each conductivity data point was assigned to the mean temperature $T = T_{top} + \frac{T}{2}$, and a corresponding curvature correction¹ was applied to correct for the use of a finite Q and T .

and a corresponding curvature correction¹ was applied to correct for the use of a finite Q and T .

RESULTS AND DISCUSSIONS

The resistivity at SVP is plotted versus t in Fig. 1 for two different values of L . The data show the effect of confinement, with the smallest size showing the greatest rounding of the transition and the greatest increase of $\rho(t = 0)$.

The scaling variable F (Eq. 1) is plotted versus X (Eq. 2) for the two sizes in Fig. 2. Except perhaps for $X \leq -2$, the data collapse onto a single curve, thus supporting the concept of finite-size

scaling. It is difficult to tell whether the small difference in F between the two data sets below $X \cong -2$ is significant or due to unknown systematic experimental errors.

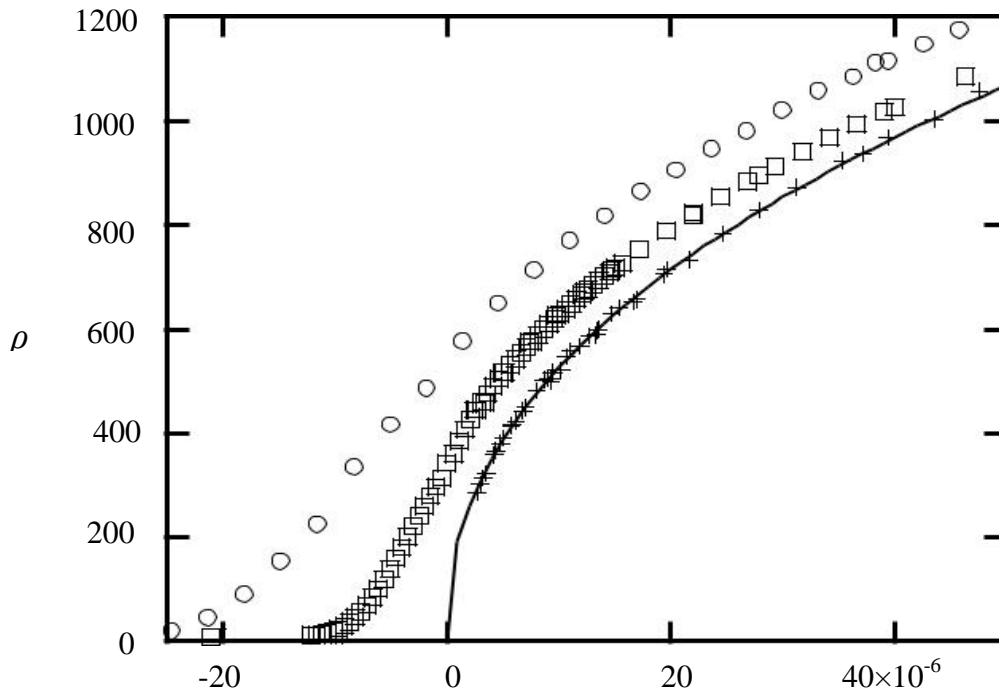


Figure 1: Thermal resistivity versus reduced temperature at SVP for $L = 0.5\mu\text{m}$ (open circles) and $1.0\mu\text{m}$

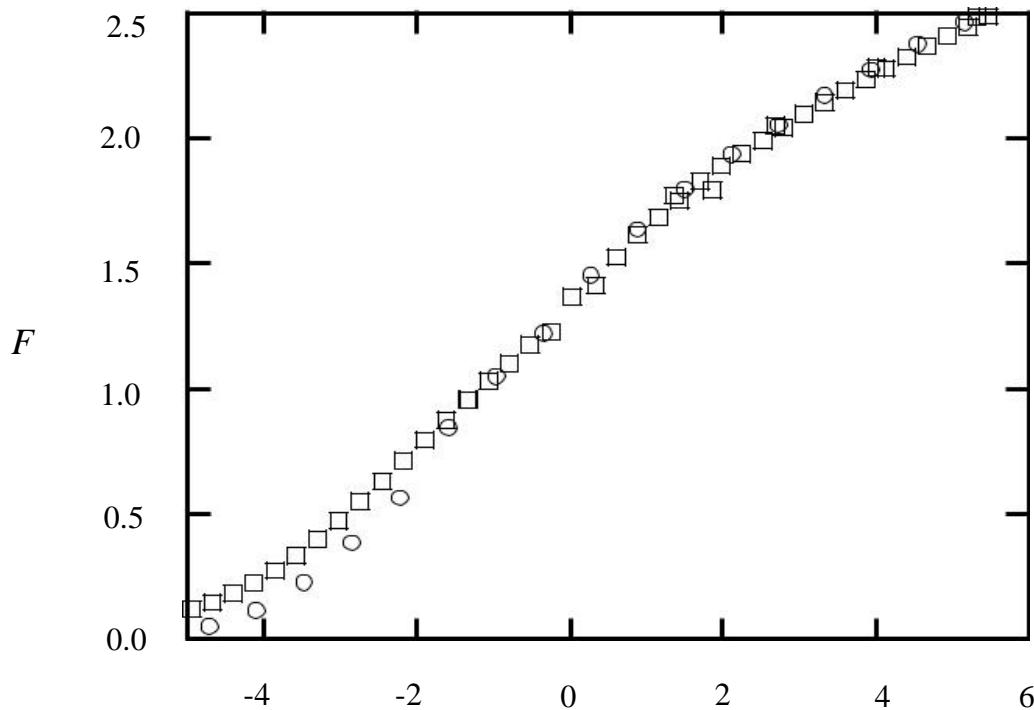


Figure 2: F versus X at SVP for $L = 0.5\mu\text{m}$ (open circles) and $1.0\mu\text{m}$.

Figure 3 shows $\rho(t, P, L)$ as a function of t for six different values of P and $L = 1.0\mu\text{m}$. The resistivity does not drop to zero below $t = 0$, as is the case for the bulk fluid¹. The value of $\rho(t = 0, P, L)$ varies by nearly a factor of three for the pressures used.

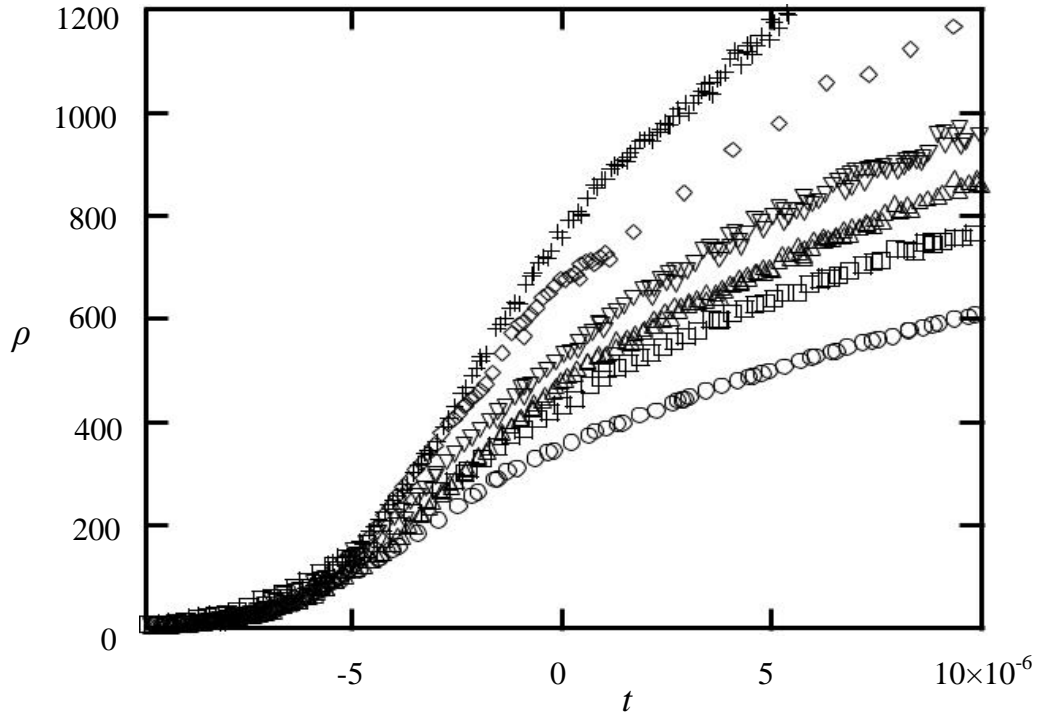


Figure 3: Thermal resistivity versus reduced temperature for $L=1.0\mu\text{m}$ at SVP

In Fig.4 the function F is plotted versus X for six different pressures. Within our resolution the data collapse on the same curve, suggesting that a single scaling function describes all six pressures. The collapse occurs despite the large variation of ρ at constant t .

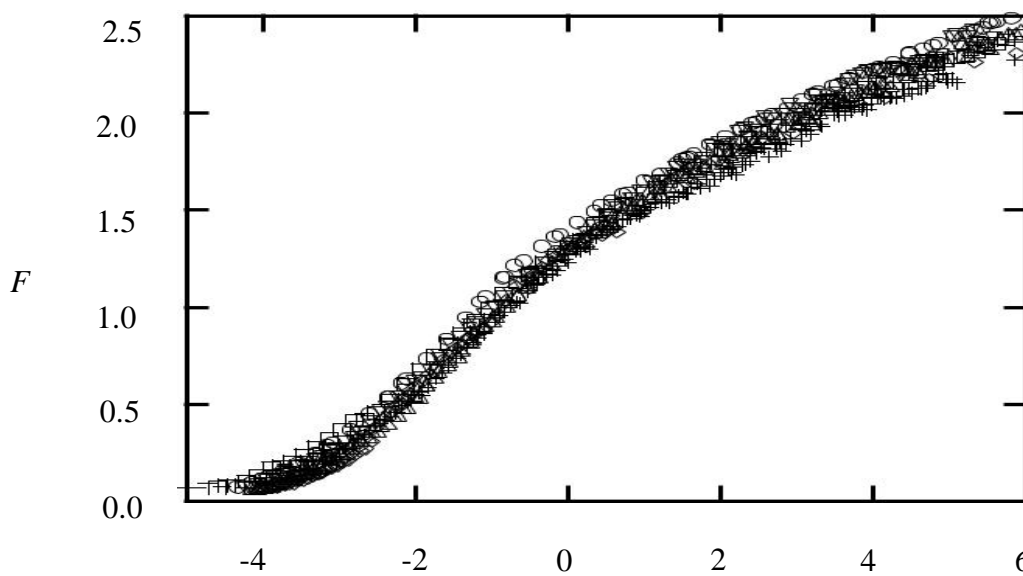


Figure 4: Scaling function F versus scaling $X = \ln(\rho(t, P, L) - \rho(t = 0, P, L))$ for $L = 1.0\mu\text{m}$ at SVP (open circles)

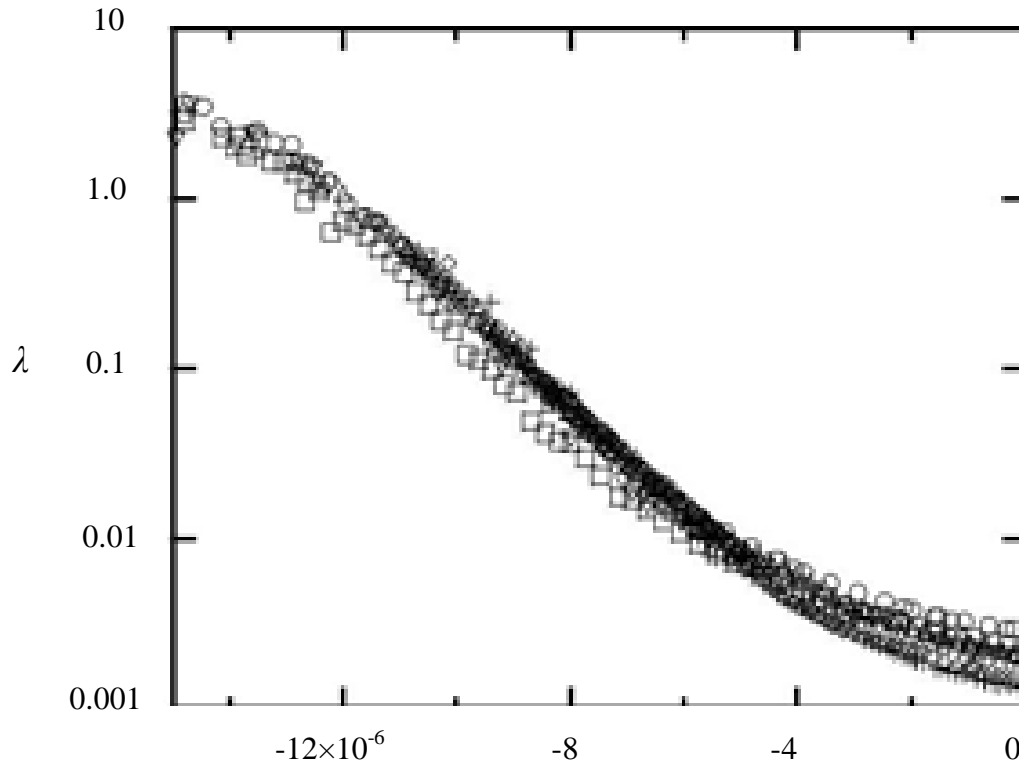


Figure 5: The thermal conductivity below T_λ on a logarithmic scale versus reduced temperature on a linear scale for $L = 1.0\mu\text{m}$ at SVP (open circles).

The thermal conductivity λ is plotted on a logarithmic scale versus t on a linear scale in Fig. 5 for temperatures below $T_\lambda(P)$. It is consistent with an exponential growth below $T_\lambda(P)$ as noted previously³. The amplitudes and arguments of the exponential are approximately the same for all pressures. These results suggest that λ , rather than the scaling function F , is independent of pressure in this temperature region, and that universality breaks down below $T_\lambda(P)$.

Aside from testing scaling and universality, an important issue is to what extent detailed theoretical calculations can reproduce the conductivity. As discussed above, the theoretical information is limited. Monte Carlo calculations, which give the shape of the scaling function quite well, involve as yet undetermined parameters. However, the recent renormalization group calculations have yielded results for λ at SVP⁴.

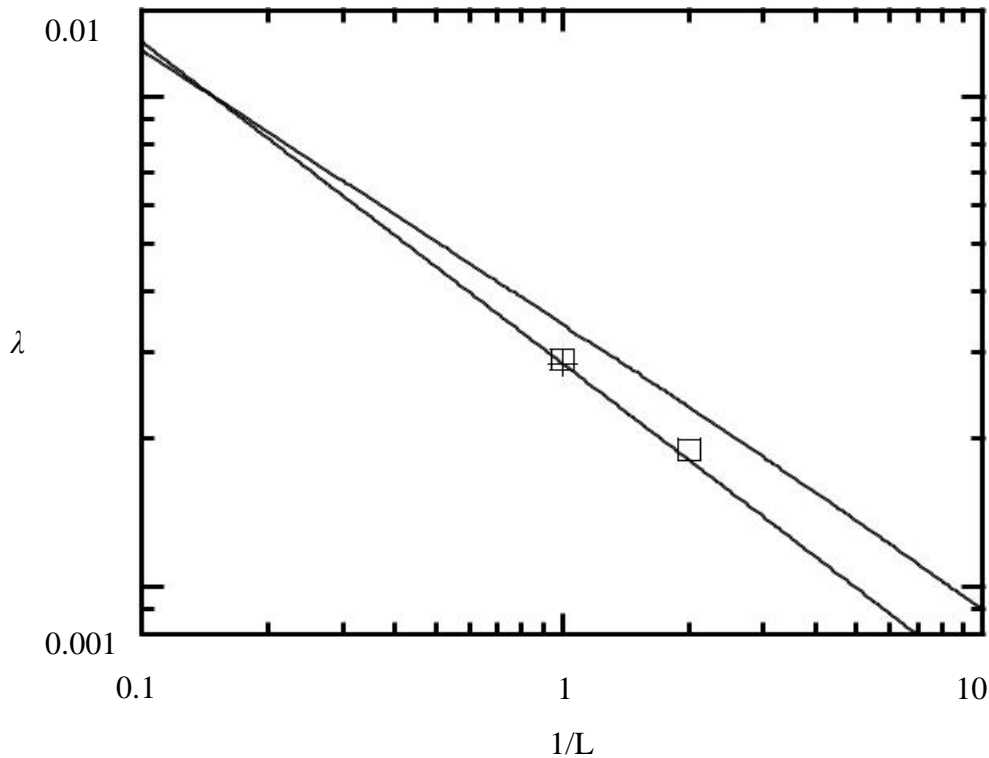


Figure6: Thermal conductivity $\lambda(t = 0)$ vs L^{-1} on logarithmic scales.

In Fig.6 we show data for $\lambda(t = 0)$ as a function of L^{-1} on logarithmic scales. The phenomenological scaling function Eq. (1) predicts $\lambda(t = 0) \propto L^{-x/\nu}$ which, for $x/\nu = 0.656$ is shown by the dashed straight line. The RG prediction is given by the solid line (note that the horizontal axis differs from the original; here, L is the radius of the channel, not the diameter). Although it comes modestly close to the data points, it does not follow a pure power law, as manifested by curvature of the solid line in the figure. Near $L \approx 1$ the effective exponent (i.e. the local slope of the line in Fig. 6 is close to 0.56, which differs significantly from the prediction based on Eq. 1. Although the data points tend to favor the larger exponent x/ν , they do not cover a sufficient range of L to be decisive. Future plans call for the measurement of the resistivity at larger L , with the largest ($50\mu\text{m}$) to be flown on the International Space Station, extending the range covered to two decades in L ¹⁰.

TABLE 1 Values of the parallel conductance C_w and scaling function F at $X=0$ versus P

Cell	L (μ m)	P (bar)	ξ_0 (nm)	$10^{-4} \rho_0$ (cmK/W)	x	$10^{-4} C_{0w}$ (W/K)	$F(0)$
II	0.5	SV P	0.1432	8.312	0.4397	13.3	1.35
II	1	SV P	0.1432	8.312	0.4397	10.5	1.35
I	1	SVP	0.1432	8.312	0.4397	9.35	1.40
I	1	6.95	0.1425	9.073	0.4251	8.81	1.30
I	1	11.25	0.1410	10.19	0.4250	8.41	1.30
I	1	14.73	0.1399	11.10	0.4250	8.07	1.32
I	1	22.31	0.1382	12.79	0.4159	7.44	1.31

CONCLUSION

In conclusion, we present quantitative study of the thermal resistivity $\rho(t, P, L)$ near the superfluid transition of He-4 at saturated vapor pressure and confined in cylindrical geometries with radii $L = 0.5$ and $1.0 \mu\text{m}$ ($t \equiv T/T_\lambda - 1$). For $L = 1.0 \mu\text{m}$, measurements at six pressures P are presented. At and above T_λ the data are consistent with a universal scaling function valid for all P .

REFERENCES

1. W. Tam and G. Ahlers, "Thermal conductivity of ^4He I from near T_λ to 3.6 K and vapor pressure to 30 bars" Phys. Rev. B 1985; 32: 5932-5958.
2. K. Nho and E. Manousakis, "Scaling of thermal conductivity of helium confined in pores" Phys. Rev. B 2001; 64(1-5): 144513.
3. A. Kahn and G. Ahlers, "Thermal Conductivity of ^4He near the Superfluid Transition in a Restricted Geometry" Phys. Rev. Lett. 1995; 74: 944-947.
4. M. Töpler and V. Dohm, "Finite-size effects on the thermal conductivity of ^4He near T_λ " Physica B 2002; 329: 200-201.
5. V. Dohm, R. Folk, "Nonlinear Dynamic Renormalization-Group Analysis above and below the Superfluid Transition in ^4He " Phys. Rev. Lett. 1981; 46: 349-352.

6. G. Ahlers, "Effect of the Gravitational Field on the Superfluid Transition in He⁴" Phys. Rev. 1968; 171: 275-282.
7. G. Ahlers, "Some aspects of the effect of gravity on the superfluid transition in ⁴He" J. Low Temp. Phys. 1991; 84; 173-195.
8. K. Mueller, G. Ahlers, and F. Pobell, "Thermal expansion coefficient, scaling, and universality near the superfluid transition of ⁴He under pressure" Phys. Rev. B 1976; 14: 2096-2118.
9. G. Straty and E. Adams, "Highly Sensitive Capacitive Pressure Gauge" Rev. Sci. Instrum. 1969; 40: 1393-1397.
10. K. Kuehn, S. Mehta, H. Fu, E. Genio, D. Murphy, F. Liu, Y. Liu, and G. Ahlers, "Singularity in the Thermal Boundary Resistance between Superfluid ⁴He and a Solid Surface" Phys. Rev. Lett. 2002; 88(1-4): 095702.